Polar Meteorol. Glaciol., **15**, 67–77, 2001

Number-size distributions of atmospheric aerosol particles ($10 < D_p < 365$ nm) at Ny-Ålesund, Norwegian Arctic: Their relationship with air mass history

Chiharu Nishita[1], Kazuo Osada[1], Keiichiro Hara[1,2], Mizuka Kido[1], Makoto Wada[2], Takashi Shibata[1] and Yasunobu Iwasaka[1]

[1]*Solar Terrestrial Environment Laboratory, Nagoya University, Furo-cho, Chikusa-ku, Nagoya 464-8601*

[2]*National Institute of Polar Research, Kaga 1-chome, Itabashi-ku, Tokyo 173-8515*

Abstract: Number-size distributions of aerosol particles between 10 and 365 nm in diameter were observed at Ny-Ålesund, Norwegian Arctic from 18 to 29 February 2000 together with concentrations of SO_2 and NH_3, and Na^+ and non-sea-salt SO_4^{2-} in non-size-segregated particles. The observed particle size distributions and concentrations were fitted by lognormal distributions and interpreted with respect to air mass histories that have different origins. Maximum concentration of aerosol particles was predominantly found in the accumulation range ($150 < D_p < 200$ nm) for all times except for air masses influenced by local air pollution. Concentrations of SO_2 and SO_4^{2-} correlated well with concentrations of aerosol particles in the accumulation range. The number-size distributions of aerosol particles in Arctic air masses derived from industrialized regions in mid-latitudes through the ice packed Arctic Ocean showed an interesting feature, a bimodal pattern with modes at Aitken and accumulation size range. Number concentrations of particles in the air masses from the North Atlantic Ocean were lower than that in air masses from other regions.

1. Introduction

The Earth's atmospheric radiation balance is influenced by aerosol particles directly through scattering and absorbing solar radiation and indirectly through acting as cloud condensation nuclei (CCN) (Charlson *et al.*, 1992; Charlson and Heintzenberg, 1995; Cox *et al.*, 1995; Meehl *et al.*, 1996). However, knowledge about physical and chemical properties of aerosol particles is still not complete enough to quantify the effect of anthropogenic aerosols. It is necessary to accumulate and update experimental data about aerosols on scales from microphysical to global as input into global climate models in order to estimate potential effect of aerosol particles. Especially, observation in polar regions is important because feedback processes are known to cause amplification of aerosol forcing at high latitudes (Blanchet, 1995).

The Arctic atmosphere is characterized by the Arctic Haze phenomenon in winter and spring. Arctic Haze has been investigated for the last three-decades (*e.g.* Shaw, 1995; Sturges, 1991), and the general features of Arctic Haze are well known. These investigations show that anthropogenic pollutants (*e.g.* SO_2, SO_4^{2-}, heavy metals and

soot) were transported several thousand kilometers from industrialized regions in mid-latitude (Russia, Europe, North America and etc.) to the Arctic. These pollutants were accumulated in the Arctic atmosphere and appeared as Arctic Haze mainly due to less wet removal of pollutants in winter and spring. According to previous reports, typical number-size distributions of particles in the Arctic atmosphere in winter and spring have a maximum in accumulation range between 100 and 300 nm in diameter, which is the most irremovable size range without wet depositions (Heintzenberg, 1980; Radke *et al.*, 1984; Shaw, 1984; Covert and Heintzenberg, 1993; Zaizen *et al.*, 1998). However, the size distributions that have dominant maximum or second maximum below 100 nm were also observed in winter and spring Arctic, and its magnitude below 100 nm varies with type of air mass (Shaw, 1986; Zaizen *et al.*, 1998). Although the number-size distribution is the most fundamental property to describe atmospheric aerosol particles, its variability and the relationship with air mass history in the Arctic winter and spring are not well known.

In this paper, we present aerosol number-size distributions observed in Ny-Ålesund, Norwegian Arctic, for 12 days in early spring. To characterize the air mass observed and to deduce relating precursor conditions, we observed concentrations of other constituents (SO_2, NH_3, non-sea-salt SO_4^{2-}, and Na^+) in the atmosphere. From these data, we selected several occasions of typical number-size distributions and calculated for backward air trajectories. Then, we compared the typical number-size distributions with the results of the trajectory analysis to see the relationship with air mass histories.

2. Experiment

2.1. Field Observations

Measurements of number-size distribution of atmospheric aerosol particles were carried out at Ny-Ålesund, Svalbard (78.6°N, 11.7°E) from 18 to 29 February 2000. The sun first rises above the horizon on 18 February in this latitude, but sunlight does not reach Ny-Ålesund until about 8 March because southern mountains (about 500 m asl) and glaciers inhibit direct sunlight. The observatory "Rabben" is located on a hill (about 40 m asl) approximately 1 km northwest of the town of Ny-Ålesund. Human activities such as cars, snowmobiles, airplanes, and diesel power generators are possible local sources of pollutants.

A Scanning Mobility Particle Sizer, SMPS (model 3934 manufactured by TSI) was used for aerosol number-size distribution measurements. The SMPS used here consists of a Differential Mobility Analyzer (TSI model 3071), a Condensation Particle Counter (TSI model 3022), and a computer for control of the system and data acquisition. Number-size distributions of aerosol particles were measured from 10 to 365 nm in diameter taking 90 s per scan cycle. In the data analysis, these raw data have to be integrated to ensure adequate counting statistics to obtain relative size distributions. The sample air was drawn via a 2-m long steel inlet pipe with 10-cm inner diameter at a flow rate of 600 cm^3/min. The height from the ground to the top of the inlet was 3 m. The temperature of the sample air in inlet pipe and SMPS was not controlled, and the room temperature was between 15 and 25°C. The diffusion loss of aerosol particles in the steel pipe is estimated at about 2% and 25% for particles of 100 nm and 10 nm in

diameter respectively but the data presented in this paper were not corrected for the particle loss. Air temperature, pressure, relative humidity, wind speed and direction were also measured at Rabben (Morimoto *et al.*, 2001). Aerosol particles, SO_2 and NH_3 were collected on a Teflon membrane filter (Advantech, 1.0μm pore size), alkaline and acid impregnated filters respectively to obtain chemical characteristics of aerosol particles and relating precursor gases. The detailed descriptions of sampling method were given by Hara *et al.* (1997, 1999a) and Kido *et al.* (2001).

2.2. *Aerosol size distributions*

Lognormal distribution is known as the function that provides a good fit to atmospheric aerosol size distribution, and is in common use. In general, three modes that exist in aerosol size distribution are defined as the nucleation mode in diameter range <20 nm (some times called the ultrafine mode), the Aitken mode from 20 to 100 nm, and the accumulation mode from 100 to 1000 nm. Hence, number-size distribution of aerosols can be described generally by nine parameters (Hinds, 1982; Jaenicke, 1993).

In order to describe the characteristics of arctic aerosols during the polar night, and compare to other data, we used the lognormal distribution to describe the aerosol size distributions observed. Lognormal distribution is

$$\frac{dN}{d\log D_p} = \sum_{i=1}^{n} \frac{N_i}{\sqrt{2\pi}\log\sigma_{g,i}} \exp\left[-\frac{(\log D_p - \log \overline{D_{p,i}})^2}{2\log^2 \sigma_{g,i}}\right], \quad (1)$$

where dN: the differential number concentration of aerosol particles in the size range D_p to $D_p + dD_p$, N_i: the total aerosol number concentration in mode i, $\overline{D_{p,i}}$: the geometric mean diameter, $\sigma_{g,i}$: the geometric standard deviation in each mode, and n: number of modes (Seinfeld and Pandis, 1998).

We obtained the parameters of each lognormal distribution using the least square fitting on a log-probability plot according to Hinds (1982). To calculate multimodal parameters, at first, we selected a part of the size range that dominates a single mode, then, three parameters for the first mode were estimated. The parameters of second and, if necessary, third modes were estimated from the residual portion of the size range. This fitting procedure is not automatic, rather requires trial and error to obtain the best-fit parameters.

2.3. *Backward trajectory analysis*

Isentropic backward trajectories were calculated by the model given in Sakai *et al.* (2000). The global field data compiled by Japan Meteorological Agency (JMA) was used. The initial point of the backward trajectories was above Ny-Ålesund (79°N, 12°E), 1.5 km altitude.

3. Result and discussion

Figure 1 shows temporal variations of wind direction, wind speed, air temperature, relative humidity (Morimoto *et al.*, 2001), concentrations of Na^+ and non-sea-salt

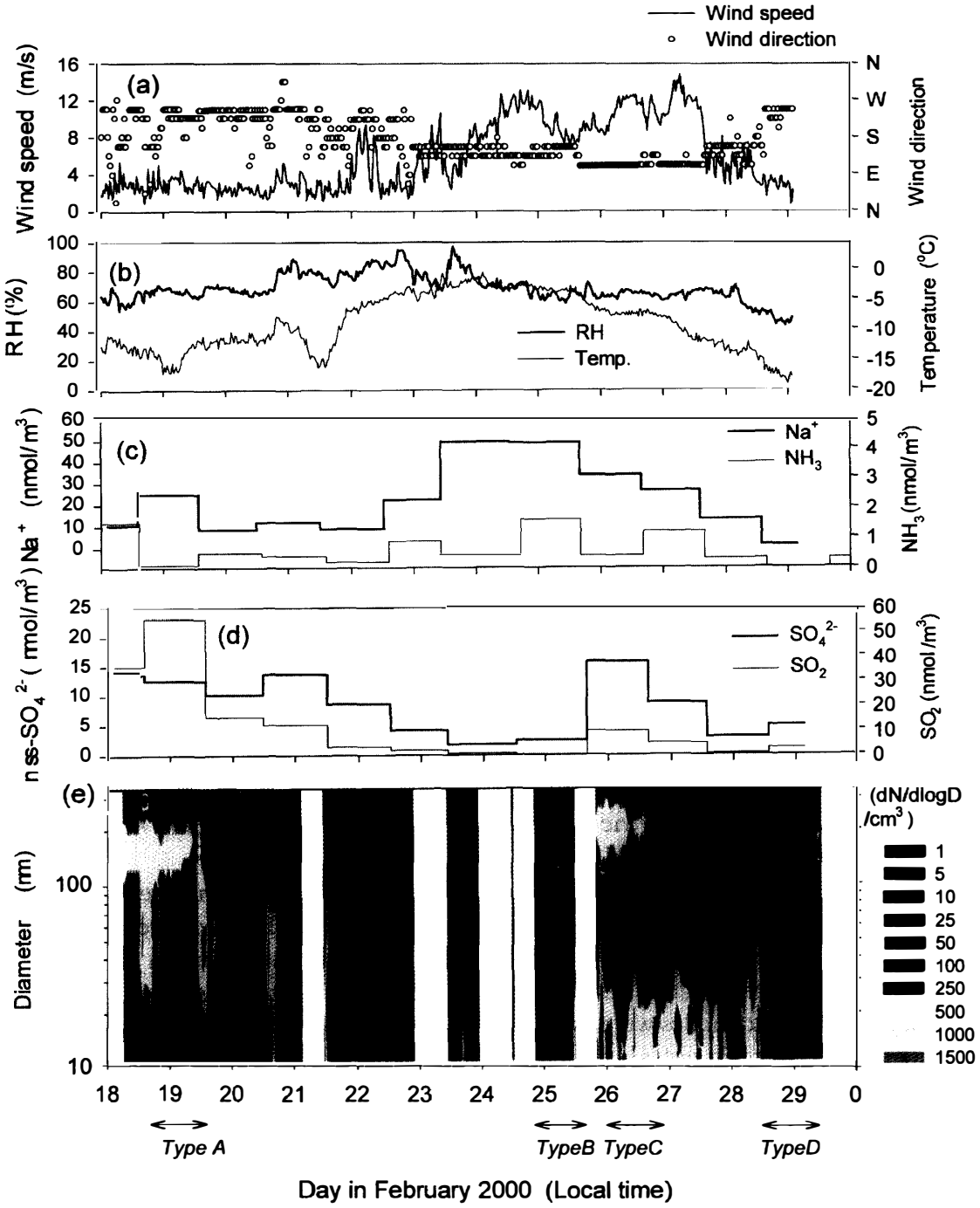

Fig. 1. Temporal variation of atmospheric parameters observed between 18 and 29 February 2000 at Rabben, Ny-Ålesund; (a) wind directions and wind speeds; (b) air temperatures, relative humidity (Morimoto et al., 2001); (c) concentrations of Na^+ and nss-SO_4^{2} in non-size-segregated aerosol particles; (d) SO_2 and NH_3 concentrations and (e) contour plots of aerosol size distributions $dN/d\log D_p$ (hourly averaged data) between 10 and 365 nm in diameter. Blank bands mean "no data". Local contamination was not removed from the data presented here. "Type A" to "Type D" at the bottom represent selected periods for typical air masses (see text).

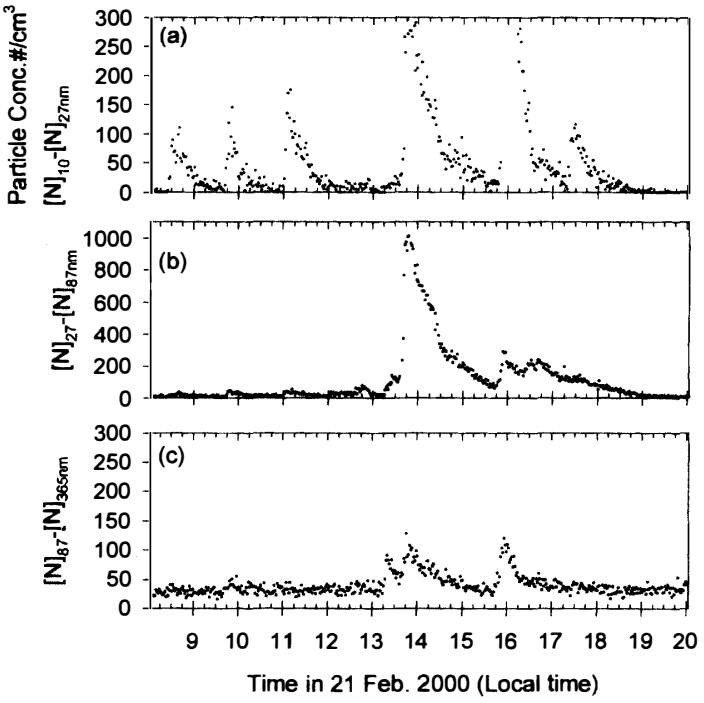

Fig. 2. Examples of spike peaks of particle concentrations observed when air was influenced by local contamination; raw data of total particle concentrations in the size range (a) $10 < D_p < 27$ nm, (b) $27 < D_p < 87$ nm, and (c) $87 < D_p < 365$ nm.

(nss-) SO_4^{2-} in aerosol particles, SO_2 and NH_3 concentrations and a contour plot of number-size distributions of particles between 18 and 29 February 2000 at Ny-Ålesund. The number-size distributions in the contour plot are made from hourly averaged data including local pollution episodes. The concentration of nss-SO_4^{2-} was calculated from the concentration of Na^+ in the sample and equivalent ratio of SO_4^{2-}/Na^+ (0.12) in seawater (Wilson, 1975).

To obtain representative characteristics of the aerosol size distribution during our study period, four short periods were selected according to Na^+ as an indicator of marine air, nss-SO_4^{2-} and SO_2 as anthropogenic pollutants, meteorological parameters, and changes of aerosol number concentrations at the Aitken and the accumulation modes. Variation of the particle concentration in the accumulation range correlates well with the concentration of nss-SO_4^{2-} and SO_2, such as high between 18 and 22 February, low in 23 and 25 February when high Na^+ concentrations were obtained. Increase of Na^+ concentration was coincident with cyclonic storm conditions of high temperature and high wind speed, suggesting that the air mass during high Na^+ concentration derived from the oceanic area to the south. To obtain the typical unpolluted condition, the data having sporadic increase of aerosol concentrations were excluded. As shown in Fig. 2, sharp peaks of the Aitken particle ($D_p < 100$ nm) concentrations were observed during local air contamination from exhausts of motor vehicles, diesel power generators, and other sources. To calculate the fitting parameters, we used only data that showed stable and constant concentrations in the Aitken and

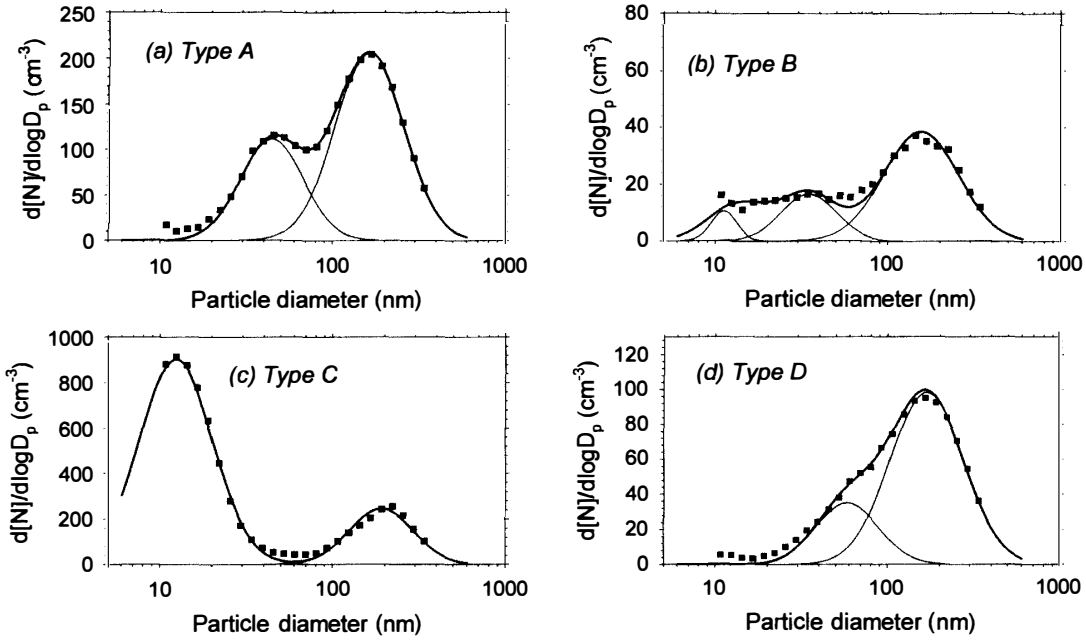

Fig. 3. Number-size distributions of aerosol particles: (a) for Type A, (b) for Type B, (c) for Type C, and (d) for Type D as the integrated and screened data during the short period shown in Fig. 1. Filled squares represent observed data. The lognormal functions fitted on each mode and the sums of them are indicated as doted line and solid line, respectively.

nucleation size ranges. About 75% of the total data set survived after peak screening for local contamination.

Figures 3a to 3d show the average size distributions for the period indicated at the bottom of Fig. 1 as Type A to D. The parameters of size distribution fitted as the sum of the lognormal distributions are summarized in Table 1. The five days backward air trajectories for the period of type A to D were presented in Figs. 4a to 4d.

The aerosol number-size distribution of Type A (Fig. 3a) shows a bimodal distribution with a clear dip at about 70 nm and with higher number density at the accumulation mode. The concentrations of SO_2 and nss-SO_4^{2-} were high in Type A. The backward trajectory for Type A (Fig. 4a) indicates that the air parcel had passed over an industrialized region in northwestern Siberia which is a major source region of Arctic haze (Sturges, 1991).

During the period of Type B, air temperature was high, Na^+ concentration was the highest in this observation, and concentrations of nss-SO_4^{2-} and SO_2 were very low. The air mass for Type B is from the North Atlantic Ocean (Fig. 4b). As indicated by high Na^+ concentration and the air trajectory, the characteristics of aerosol chemistry and the size distribution for Type B would be influenced by open sea areas such as the Norwegian Sea and the North Atlantic Ocean. The size distribution of Type B was fitted as the sum of trimodal lognormal distributions. However, the Aitken and nucleation modes were not clearly distinguished as separate modes because the concentration below 50 nm was quite low. Regarding the concentration of accumulation mode of Type B, the clean oceanic air mass was five times as clean as in the polluted air

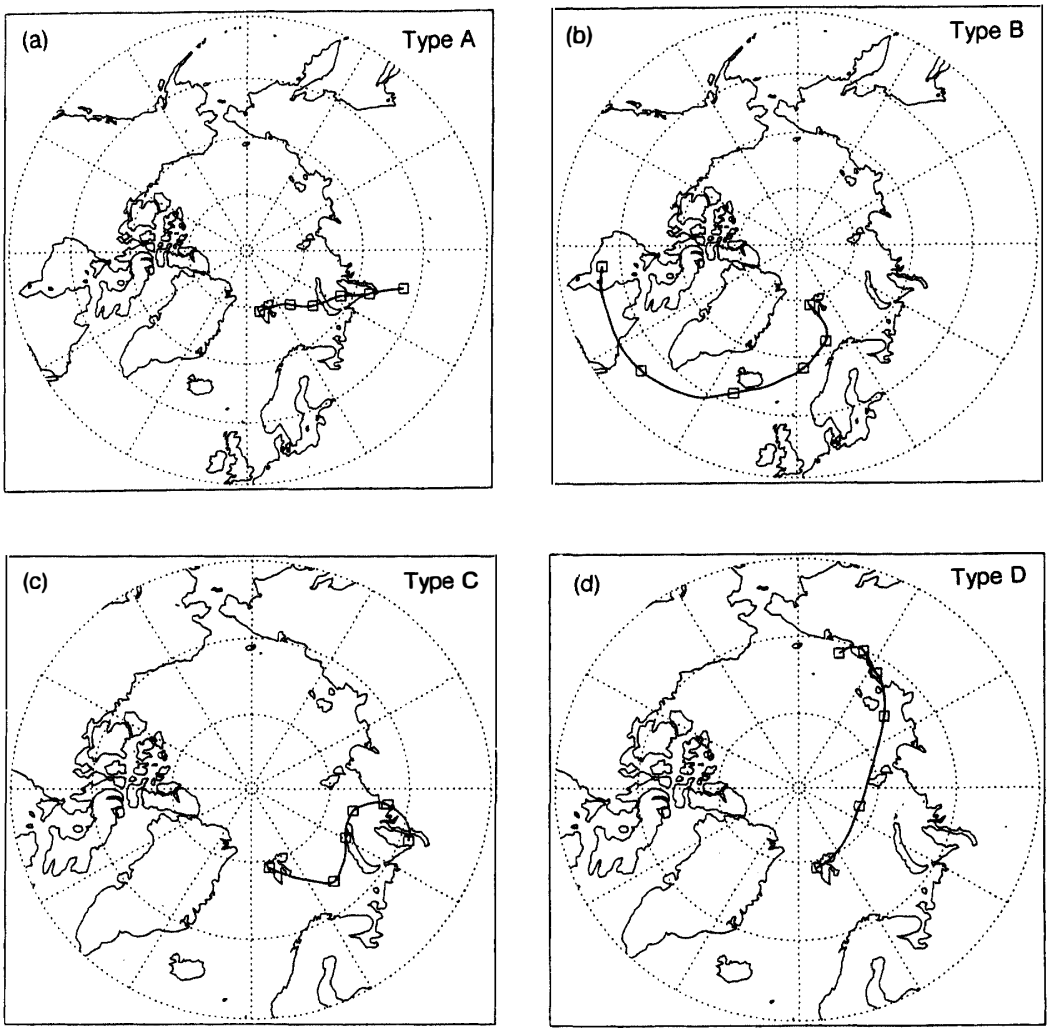

Fig. 4. Air mass back ward trajectory from Ny-Ålesund for the period of (a) Type A, (b) Type B, (c) Type C, and (d) Type D. The squares represent an interval of 24 hours.

mass of Type A.

The concentrations of particles in the nucleation mode (about 15 nm) increased rapidly on 25 February as the local wind direction changed to east-southeast at Rabben, and kept high values for about three days. In this period, the aerosol size distributions were quite different from the others, which were continuously dominated by very high concentrations of the nucleation mode between 10 and 20 nm (Fig. 3c). Ultra-fine particles in the nucleation mode coagulate rapidly to Aitken particles; their lifetime in the atmosphere is considered to be shorter than a day. Then these imply the steady contribution of anthropogenic air pollution that have to be local rather than long-range transport because of short lifetime of ultra-fine particles of the nucleation mode. The power plant at Ny-Ålesund, which was 1.3 km in the windward direction from the observation site, is considered the source of the ultra-fine particles in this case. Longyearbyen, the biggest town in Svalbard, might be another possible source; it is about 100 km southeast of Ny-Ålesund. Indeed, the backward air trajectory (Fig. 4c)

Table 1. Parameters of lognormal fitting of the aerosol size distributions for Type A to Type D observed at Ny-Ålesund in February 2000.

	Type A	Type B	Type C	Type D
		Nucleation mode		
$N_{\text{nucleation}}$ (cm^{-3})	—	6	481	—
$\overline{D_{p,\ nucleation}}$ (nm)	—	14	12	—
$\log \sigma_{g,\ nucleation}$	—	0.17	0.21	—
		Aitken mode		
N_{Aitken} (cm^{-3})	51	7	—	16
$\overline{D_{p,\ Aitken}}$ (nm)	44	35	—	58
$\log \sigma_{g,\ Aitken}$	0.18	0.16	—	0.18
		Accumulation mode		
$N_{\text{accumulation}}$ (cm^{-3})	103	21	115	53
$\overline{D_{p,\ accumulation}}$ (nm)	163	154	191	169
$\log \sigma_{g,\ accumulation}$	0.20	0.22	0.19	0.21

showed that an air mass moved above Longyearbyen about 3 hours before arriving at the sampling site.

In the last case, the size distribution of Type D (Fig. 3d) was also dominated by the accumulation mode with a shoulder of the Aitken mode. The air temperature during Type D was cold but the concentrations of nss-SO_4^{2-} and SO_2 were low. Moreover, the Na^+ concentration was also low during Type D. The backward air trajectory (Fig. 4d) shows that the air parcel was traveling over sea ice from the coast of the East Siberian Sea, where there are no significant pollutant sources (Fukasawa *et al.*, 1997) via the Arctic Ocean for five days until arrival at Ny-Ålesund. The number concentration in the accumulation mode in Type D was lower than that in Type A from northwestern Siberia (Fig. 4a), and higher than Type B from the Atlantic Ocean (Fig. 4b). Comparing with Type A (Fig. 4a), the geometric mean diameter (GSD) of Aitken mode in Type D is slightly larger. Since the air mass of Type D was not influe nced by anthropogenic source during the past five days, it may carry well-aged aerosols. Aitken particles are considered to grow via coagulation with ultra-fine particles and condensation of H_2SO_4 from precursor gases as time passes; some larger Aitken particles (about 70 nm) may also grow via cloud processing (Hoppel *et al.*, 1986; Hoppel *et al.*, 1994a, b) to the accumulation particles (see review for Raes *et al.*, 1995). The difference of the geometric mean diameter for the Aitken mode between Types A and D might reflect aging time during transport in the Arctic region after contact with anthropogenic pollution.

Aerosol concentrations in the nucleation range were insignificant except for the short-term increase of the local pollution episodes (Type C). Presence of particles in the range between about 10 and 20 nm implies that active new particle formation by homogenous nucleation of precursor gases occurred in the neighborhood. Gas phase oxidation of SO_2 to H_2SO_4 gas needs OH radicals formed by photolysis of O_3 with ultraviolet radiation. During the dark polar night, natural new particle formation by homogenous nucleation from gaseous H_2SO_4 must be very limited. For the semi-dark

period like this study, rapid transport of the air mass exposed to sunlight might allow the existence of a weak nucleation mode as found in Type B. Results in sunlit Arctic summer and autumn (Covert *et al.*, 1996) showed tri-modal size distribution with a clear nucleation mode.

As described above, atmospheric conditions of the dark polar night and semi-dark period are not suitable for new particle formation by homogeneous nucleation; thus, the predominant mode in aerosol size distribution without local pollution was the accumulation mode. Our data as well as old data obtained in spring at Ny-Ålesund (Covert and Heintzenberg, 1993) showed similar size distribution having the GSD about 200 nm for the accumulation mode.

On the other hand, although data are limited, slightly smaller mode diameter (about 100 nm) for the accumulation mode has been reported for Antarctic winter to early spring (July-September) season (Gras, 1993; Okada *et al.*, 1990). If meteorological and gaseous precursor conditions were similar in both Polar Regions, a similar size distribution would be expected. However, the GSD of the accumulation mode at Ny-Ålesund in the semi-dark period was almost double. Although the difference in the conditions of aerosol size measurements may inhibit a precise comparison of the GSD, difference of SO_2 concentration may form a dissimilarity in the GSD of the accumulation mode between the Arctic and the Antarctic locations. In the Arctic winter and spring, SO_2 concentration converted to SO_4^{2-} as accumulation particles is high but its concentration should be very low in Antarctica due to the pristine natural environment without anthropogenic pollution with SO_2. Indeed, SO_2 concentrations at Syowa station in winter were about 1/10 (or less) of the value at Ny-Ålesund (Hara *et al.*, 1999b).

4. Summary and conclusions

Aerosol number-size distributions in the size range from 10 nm to 365 nm were measured with concentrations of trace constituents (SO_2, NH_3, nss-SO_4^{2-}, and Na^+) in Ny-Ålesund, Norwegian Arctic, for 12 days in February 2000. We selected several periods for typical aerosol size distributions and identified the origins of air masses, such as marine, industrialized continent, and the Arctic, by the concentrations of trace constituents and trajectory analysis. Observed size distributions can be fitted accurately by lognormal distributions, and statistical parameters of size distributions were obtained.

The structures of the aerosol size distributions were different according to the history and origin of the air mass. The aerosol particles transported from industrialized continental region were bimodal size distributions with Aitken and accumulation modes. The distribution of aerosol particles from the Arctic region was also a bimodal pattern, but the mean diameter of Aitken mode was slightly larger than that of the aerosols from industrialized regions. This may reflect the difference of aging time during transport in the Arctic atmosphere. Compared with the other types, total particle concentration was quite low in the marine air mass, suggesting active wet deposition in the marine region and fewer precursors. Nucleation mode ($D_p < 20$ nm) was insignificant in the observed aerosol distributions except for the case of local

contamination.

Acknowledgments

The authors would like to thank Dr. M. Shiobara, Mr. N. Hirasawa, Mr. M. Watanabe, and the staff members of the National Institute of Polar Research for their assistance in the observations, and staff members of Kings Bay for help in staying at Ny-Ålesund. We are grateful to Dr. T. Sakai for helping with the air mass backward trajectory analysis. The Ministry of Education, Arts and Culture, Japan, supported this work as part of a Grant-in-Aid for International Scientific Research Program, 09041104.

References

Blanchet, J.-P. (1995): Mechanisms of direct and indirect climate forcing by aerosols in the Arctic region. Aerosol Forcing of Climate, ed. by R.J. Charlson and J. Heintzenberg, Chichester, J. Wiley, 109–121.

Charlson, R.J. and Heintzenberg, J. (1995): Aerosol Forcing of Climate. Chichester, J, Wiley, 416 p.

Charlson, R.J., Shwartz, S.E., Hales, J.M., Cess, R.D., Coakley, J.A., Hansen, J.E. and Hoffmann, D.J. (1992): Climate forcing by anthropogenic aerosols. Science, **255**, 423–430.

Covert, D.S. and Heintzenberg, J. (1993): Size distributions and chemical properties of aerosol at Ny-Ålesund, Svalbard. Atmos. Environ., **17/18**, 2989–2997.

Covert, D.S., Wiedensohler, A., Aalto, P., Heintzenberg, J., McMurry, P.H. and Leck, C. (1996): Aerosol number size distributons from 3 to 500 nm diameter in the arctic marine boundary layer during summer and autumn. Tellus, **48B**, 197–212.

Cox, S.J., Wang, W.-C. and Schwartz, S.E. (1995): Climate response to radiative forcing by sulfate aerosols and greenhouse gases. Geophys. Res. Lett., **22**, 2509–2512.

Fukasawa, T., Ohta, S., Murao, N., Yamagata, S. and Makarov, V.N. (1997): Aerosol observations in the Siberian Arctic. Proc. NIPR Symp. Polar Meteorol. Glaciol., **11**, 150–160.

Gras, J.L. (1993): Condensation nucleus size distribution at Mawson, Antarctica: Microphysics and chemistry. Atmos. Environ., **9**, 1427–1434.

Hara, K., Osada, K., Hayashi, M., Matsunaga, K. and Iwasaka, Y. (1997): Variation of concentration of sulfate, methanesulfonate and sulfur dioxide at Ny-Ålesund in 1995/96 winter. Proc. NIPR Symp. Polar Meteorol. Glaciol., **11**, 127–137.

Hara, K., Osada, K., Hayashi, M., Matsunaga, K., Shibata, T. and Iwasaka, Y. (1999a): Fractionation of inorganic nitrates in winter Arctic troposphere: Coarse aerosol particles containing inorganic nitrates. J. Geophys. Res. **104**, 23671–23679.

Hara, K., Osada, K., Kido, M., Matsunaga, K., Iwasaka, Y., Yamanouchi, T., Hashida, G., Hayashi, M. and Fukatsu, T. (1999b): Variations of acidic gas concentrations at Syowa Station, Antarctica. The 20th Symposium on Polar Meteorology and Glaciology, Program and Abstracts, 9–10, December 8–9, 1999. Tokyo, National Institute of Polar Research, 9–10.

Hinds, W.C. (1982): Chapter 4 Particle size statistics. Aerosol Technology. New York, J. Wiley, 69–103.

Heintzenberg, J. (1980): Particle size distribution and optical properties of Arctic haze. Tellus, **32**, 251–260.

Hoppel, W.A., Frick, G.M. and Larson, R.E. (1986): Effect of nonprecipitating clouds on the aerosol size distribution in the marine boundary layer. Geophys. Res. Lett., **13**, 125–128.

Hoppel, W.A., Frick, G.M., Fitzgerald, J.W. and Larson, R.E. (1994a): Marine boundary layer measurements of new particle formation and the effects of nonprecipitating clouds have on aerosol size distribution. J. Geophys. Res., **99**, 14443–14459.

Hoppel, W.A., Frick, G.M., Fitzgerald, J.W. and Wattle, B.J. (1994b): A cloud chamber study of the effect that nonprecipitating water clouds have on the aerosol size distribution. Aerosol Sci. Technol., **20**, 1–30.

Jaenicke (1993): Tropospheric Aerosols, Aerosol-Cloud-Climate Interactions, ed. by P.V. Hobbs. San Diego, Academic Press, 1–31.

Kido, M., Osada, K., Matsunaga, K. and Iwasaka, Y. (2001): Temporal change in ammonium/sulfate ratios for free tropospheric aerosols from early winter to spring at a high elevation site in the Japanese Alps. J. Environ. Chem., **1**, 33–41.

Meehl, G.A., Washington, W.M., Erickson, III, D.J., Briegleb, B.P. and Jaumann, P.J. (1996): Climate change from increased CO_2 and direct and indirect effects of sulfate aerosols. Geophys. Res. Lett., **23**, 3755–3758.

Morimoto, S., Aoki, S., Wada, M. and Yamanouchi, T. (2001): Meteorological data at Japanese Ny-Ålesund Observatory, Svalbard, in 1999 and 2000. submitted to NIPR Arct. Data Rep., **5**.

Okada, K., Aoki, T., Ikegami, M., Zaizen, Y. and Ito, T. (1990): Aitken sulfuric-acid particles in the Antarctic atmosphere. Aerosols: Science, Industry, Health and Environment; **2**, Proceedings of the Third International Aerosol Conference, Kyoto, 1990, ed. by S. Masuda and K. Takahashi. Tokyo, Pergamon.

Radke, L.F., Lyons, J.H., Hegg, D.A., Hobbs, P.V. and Bailey, I.H. (1984): Airborne observations of arctic aerosols. I: Characteristics of Arctic haze. Geophys. Res. Lett., **11**, 393–396.

Raes, F., Wilson, J. and Van Dingenen, R. (1995): Aerosol dynamics and its implication for the global aerosol climatology. Aerosol Forcing of Climate, ed. by R.J. Charlson and J. Heintzenberg. Chichester, J. Wiley, 153–169.

Sakai, T., Shibata, T., Kwon, S., Kim, Y., Tamura, K. and Iwasaka, Y. (2000): Free tropospheric aerosol backscatter, depolarization ratio, and relative humidity measured with Raman lidar at Nagoya in 1994–1997: contributions of aerosols from the Asian continent and the Pacific Ocean. Atmos. Environ., **34**, 431–442.

Seinfeld, J.H. and Pandis, S.N. (1998): Atmospheric Chemistry and Physics: From Air Pollution to Climate Change. New York, J. Wiley, 1326.

Shaw, G.E. (1984): Microparticle size spectrum of Arctic haze. Geophys. Res. Lett., **11**, 409–412.

Shaw, G.E. (1986): Aerosols in Alaskan air masses. J. Atmos. Chem., **4**, 157–171.

Shaw, G.E. (1995): The arctic haze phenomenon. Bull. Am. Meteorol. Soc., **76**, 2403–2413.

Sturges, W.T. (1991): Pollution of the Arctic Atmosphere. Oxford, Elsevier Applied Science Publishers.

Wilson, T.R.S. (1975): Salinity and major elements of sea water. Chemical Oceanography, ed. by J.P. Riley and G. Skirrow. San Diego, Academic Press, 365–438.

Zaizen, Y., Okada, K., Ikegami, M., Aoki, T., Sawa, Y., Nishio, F. and Tachibana, Y. (1998): Size distribution of aerosols at Barrow in Alaska—A case study in spring. Polar Meteorol. Glaciol., **12**, 40–48.

(Received May 2, 2001; Revised manuscript accepted June 21, 2001)